



Natural Resources
Canada

Ressources naturelles
Canada

**GEOLOGICAL SURVEY OF CANADA
OPEN FILE 7848**

**Geological and geochemical data from the
Canadian Arctic Islands. Part XIII: new bulk
geochemical and Rock-Eval data from Upper Paleozoic cores
and preliminary results for basinal shales**

P. Kabanov and K. Dewing

2015



**GEOLOGICAL SURVEY OF CANADA
OPEN FILE 7848**

Geological and geochemical data from the Canadian Arctic Islands. Part XIII: new bulk geochemical and Rock-Eval data from Upper Paleozoic cores and preliminary results for basinal shales

P. Kabanov and K. Dewing

2015

© Her Majesty the Queen in Right of Canada, as represented by the Minister of Natural Resources Canada, 2015

doi:10.4095/296803

This publication is available for free download through GEOSCAN (<http://geoscan.nrcan.gc.ca/>).

Recommended citation

Kabanov, P. and Dewing, K., 2015. Geological and geochemical data from the Canadian Arctic Islands. Part XIII: new bulk geochemical and Rock-Eval data from Upper Paleozoic cores and preliminary results for basinal shales; Geological Survey of Canada, Open File 7848, 1 .zip file. doi:10.4095/296803

Publications in this series have not been edited; they are released as submitted by the author.

TABLE OF CONTENTS

INTRODUCTION.....	1
FIGURE 1.....	1
FIGURE 2.....	2
MATERIAL AND METHODS.....	3
TABLE 1.....	4
Bulk-element geochemistry.....	4
Rock-Eval 6 pyrolysis.....	5
RESULTS ON SHALE SAMPLES.....	6
Lithofacies subdivision of shales.....	6
TABLE 2.....	6
FIGURE 3.....	7
FIGURE 4.....	8
FIGURE 5.....	9
Properties of organic matter based on Rock-Eval pyrolysis.....	10
FIGURE 6.....	10
FIGURE 7.....	11
FIGURE 8.....	12
TABLE 3.....	12
Geochemical results.....	13
FIGURE 9.....	14
FIGURE 10.....	15
TABLE 4.....	16
TABLE 5.....	17
TABLE 6.....	17
ACKNOWLEDGEMENTS	18
REFERENCES.....	19
LIST OF TABLES	20
LIST OF FIGURES	20
LIST OF APPENDICES	21

INTRODUCTION

This publication follows the Upper Paleozoic core study (Kabanov & Dewing, 2014) and reports on new pyrolysis and ICP-MS/ES elemental data from core samples. The goal of study was to investigate hydrocarbon source-rock and tight-reservoir prospectivity of shales from the depocenter of the Sverdrup Basin (Figures 1 and 2). In addition, a set of samples across stratigraphic unconformities encountered in cores were run for ICP-MS/ES geochemistry to develop unconformity diagnostics, paleoclimate reconstructions, and better understand the effect of high-amplitude base level falls on reservoir properties and preservation organic matter. Summary of geological context and core descriptions have been published earlier (Kabanov and Dewing, 2014).

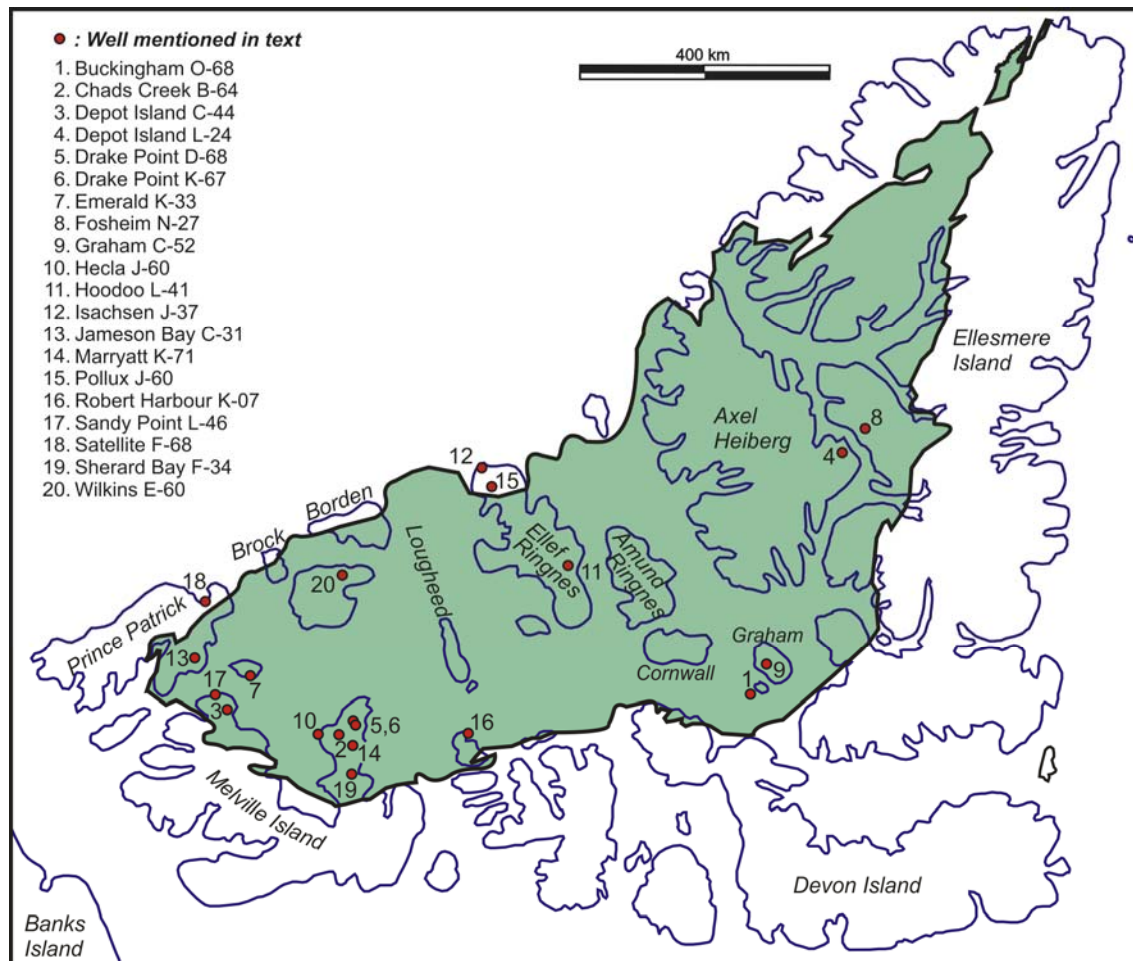


Figure 1. Locations of wells with upper Paleozoic core.

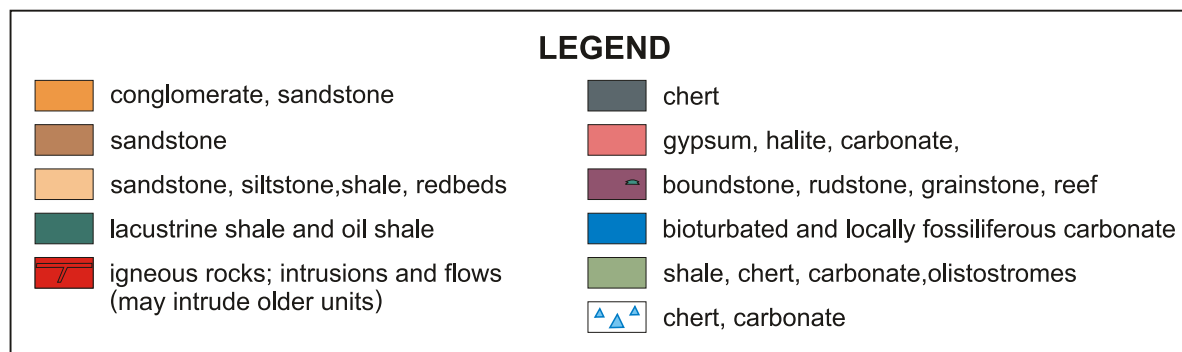
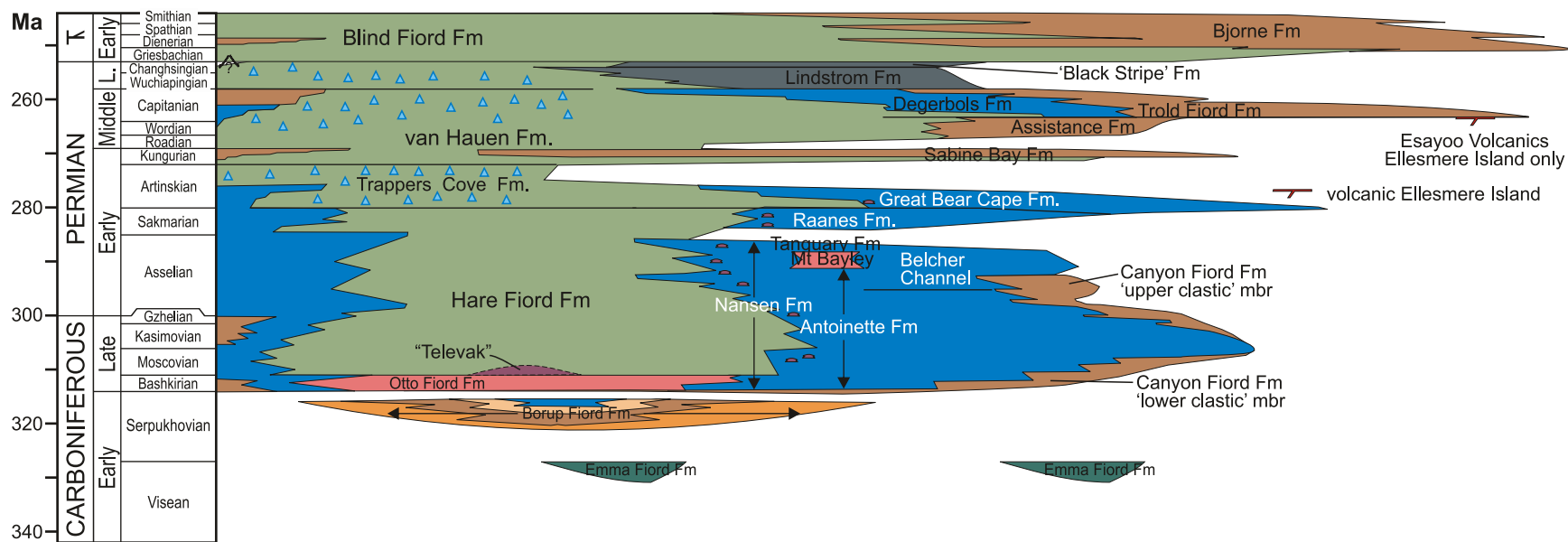


Figure 2. Stratigraphic nomenclature for the upper Paleozoic of the Canadian Arctic Islands (updated from Dewing and Embry, 2007).

MATERIAL AND METHODS

One hundred twenty-three samples were collected for geochemistry and 116 for Rock-Eval pyrolysis (Appendices 1-3). All appendices are located in the “of7848\appendix” directory. Appendix 1 is available as either a Microsoft® Office Excel® 2010 file ([appendix_1_ICP_data_Acme.xlsx](#)) or as an Adobe® PDF file ([appendix_1_ICP_data_Acme.pdf](#)). Appendix 2 is also available as either a Microsoft® Office Excel® 2010 file ([appendix_2_Rock-Eval_results.xls](#)) or as an Adobe® PDF file ([appendix_2_Rock-Eval_results.pdf](#)). Rock-Eval results compiled in Appendix 3 are available as a composite PDF file ([appendix_3_000_Rock-Eval_6_pyrograms_composite.pdf](#)) or by individual analysis as a separate PDF files (refer to the [List of Appendixes](#) for the list of individual results or navigate to the “of7848\appendix” directory to open these files. Samples were collected in 2014 with permission from the [National Energy Board \(NEB\)](#). Shaly or shale-dominated intervals in this set were represented by 97 samples. Out of these 97 samples, rocks that are described as shales and are included into analysis count 90. Only thick (2 m and thicker) shale units have been selected for this study ([Table 1](#)). Samples taken from thick (>15-20 cm) intercalations of benthic limestone and sandstone encountered in shale-dominated intervals were excluded from analysis. Shale samples were run for Rock-Eval 6 pyrolysis/combustion. The 5.5 - 7.0 gram samples were collected from core sides and loose chips. Each sample represents an averaged material collected from a stratigraphic interval exceeding 1 cm (typically 2-5 cm), to make sure that none of collected samples represents a single sedimentary lamina.

UWI	WELL SHORT NAME	TOP_DEPTH (m)	BOT_DEPTH (m)	Run (m)	RECOVERY (m)	Occurrence of shale (>2 m in thickness): red- mottled = 1; dark bioturbated (BI>2) = 2; dark laminated (BI<2) = 3	TOP_FORMATION	BOTTOM_FORMATION
300F347620108300	SHERARD BAY F-34	2667	2676.5	9.5	9.5	0	DEGERBOLS FM	DEGERBOLS FM
300F347620108300	SHERARD BAY F-33	4617	4620.1	3.1	4	0	CANYON FIORD FM	CANYON FIORD FM
300F347620108300	SHERARD BAY F-34	4620.1	4622	1.9	5	2	CANYON FIORD FM	CANYON FIORD FM
300F347620108300	SHERARD BAY F-34	5248.3	5256.5	8.2	6	0	CANYON FIORD FM	CANYON FIORD FM
300J607620110000	HECLA J-60	2598.4	2607.5	9.1	9.1	0	PERMIAN	PERMIAN
300J607620110000	HECLA J-60	3603.7	3616.5	12.8	12.8	2	VAN HAUEN FM	VAN HAUEN FM
300L677630108300	DRAKE POINT L-67	3133.3	3139.4	6.1	6	0	VAN HAUEN FM	VAN HAUEN FM
300L677630108300	DRAKE POINT L-67	3234.5	3252.5	18	17.8	0	VAN HAUEN FM	VAN HAUEN FM
300D687630108300	DRAKE POINT D-68	4677.2	4681.7	4.5	3	2	HARE FIORD FM	HARE FIORD FM
300D687630108300	DRAKE POINT D-68	4681.7	4690.6	8.9	8.1	2	HARE FIORD FM	HARE FIORD FM
300K717630108300	MARRYATT K-71	4707	4725.5	18.5	18.5	0	VAN HAUEN FM	VAN HAUEN FM
300K717630108300	MARRYATT K-71	4943	4955.5	12.5	11.6	0	BELCHER CHANNEL FM	BELCHER CHANNEL FM
300K717630108300	MARRYATT K-71	5449	5467	18	17.8	3	BELCHER CHANNEL FM	BELCHER CHANNEL FM
300B647630109300	CHADS CREEK B-64	3398.5	3399.7	1.2	0.8	0	VAN HAUEN FM	VAN HAUEN FM
300B647630109300	CHADS CREEK B-64	4586	4604.3	18.3	18.3	0	HARE FIORD FM	HARE FIORD FM
300B647630109300	CHADS CREEK B-64	5020.1	5035.9	15.8	15.5	2	HARE FIORD FM	HARE FIORD FM
300C447630114000	DEPOT ISLAND C-44	1656.9	1675.2	18.3	17.4	1	CANYON FIORD FM	CANYON FIORD FM
300C447630114000	DEPOT ISLAND C-44	2457	2465.5	8.5	8.5	0	CANYON FIORD FM	IBBETT BAY FM
300L467630115000	SANDY POINT L-46	1786.1	1795.3	9.2	9.1	0	CANYON FIORD FM	CANYON FIORD FM
300L467630115000	SANDY POINT L-46	1985.2	1988.5	3.3	3.3	0	CANYON FIORD FM	CANYON FIORD FM
300K077640104000	ROBERT HARBOUR K-07	1791.3	1800.4	9.1	9.1	0	VAN HAUEN FM	VAN HAUEN FM
300K077640104000	ROBERT HARBOUR K-07	2713.9	2721.9	8	8	2	HARE FIORD FM	HARE FIORD FM
300K337650113300	EMERALD K-33	3173.3	3179.4	6.1	6.1	0	TROLD FIORD FM	TROLD FIORD FM
300C317650116300	JAMESON BAY C-31	2404	2413.1	9.1	9.1	1	CANYON FIORD FM	CANYON FIORD FM
300D687710091000	BUCKINGHAM O-68	883	898.6	15.6	15.4	0	DEGERBOLS FM	DEGERBOLS FM
300D687710091000	BUCKINGHAM O-68	2239	2255.8	16.8	16.4	0	HARE FIORD FM	HARE FIORD FM
300D687710091000	BUCKINGHAM O-68	2758	2772	14	4.5	2	BELCHER CHANNEL FM	BELCHER CHANNEL FM
300F687720116300	SATELLITE F-68	2170.2	2173.5	3.3	3.3	0	TROLD FIORD FM	TROLD FIORD FM
300F687720116300	SATELLITE F-68	2664	2671.3	7.3	7.2	2	HARE FIORD FM	HARE FIORD FM
300F687720116300	SATELLITE F-68	3187.3	3193.4	6.1	5.2	2	HARE FIORD FM	HARE FIORD FM
300C527730090300	GRAHAM C-52	2234.8	2241.2	6.4	6.4	2	DEGERBOLS FM	DEGERBOLS FM
300C527730090300	GRAHAM C-52	2671.3	2675.2	3.9	0.9	2	HARE FIORD / BELCHER CHANNEL	HARE FIORD / BELCHER CHANNEL
300C527730090300	GRAHAM C-52	3061.7	3067.8	6.1	6.1	1	HARE FIORD / BELCHER CHANNEL	HARE FIORD / BELCHER CHANNEL
300C507750114000	BROCK C-50	1906.5	1912.6	6.1	5.3	2	DEGERBOLS FM	DEGERBOLS FM
300C507750114000	BROCK C-50	2266.2	2272.3	6.1	5.6	0	DEGERBOLS FM	DEGERBOLS FM
300C507750114000	BROCK C-50	2836.5	2842.6	6.1	6.1	2	VAN HAUEN FM	VAN HAUEN FM
300C507750114000	BROCK C-50	3326	3326.9	0.9	0.5	0	NANSEN FM	NANSEN FM
300C507750114000	BROCK C-50	3688.7	3695.1	6.4	4.4	0	NANSEN FM	NANSEN FM
300C507750114000	BROCK C-50	3959.7	3961.2	1.5	1.2	0	NANSEN FM	NANSEN FM
300E607800111000	WILKINS E-60	2782.8	2790.7	7.9	7.2	0	DEGERBOLS FM	DEGERBOLS FM
300E607800111000	WILKINS E-60	3374.1	3378.7	4.6	3.5	0	HARE FIORD FM	HARE FIORD FM
300L417820099300	HOODOO L-41	1220.4	1229.3	8.9	8.9	0	OTTO FIORD FM	OTTO FIORD FM
300L417820099300	HOODOO L-41	2836.8	2839.8	3	3	0	OTTO FIORD FM	OTTO FIORD FM
300L417820099300	HOODOO L-41	3838.7	3849	10.3	10.3	0	OTTO FIORD FM	OTTO FIORD FM
300G607910104300	POLLUX G-60	2298.8	2314	15.2	15.2	0	DEGERBOLS FM	DEGERBOLS FM
300G607910104300	POLLUX G-60	2799.3	2800.5	1.2	1.2	0	ASSISTANCE FM	ASSISTANCE FM
300G607910104300	POLLUX G-60	3368	3373.2	5.2	4.6	0	CANYON FIORD FM	CANYON FIORD FM
300G607910104300	POLLUX G-60	3423.8	3428.7	4.9	4.9	0	CANYON FIORD FM	CANYON FIORD FM
300J377920105000	ISACHSEN J-37	3183.9	3192.2	8.3	8.3	0	ASSISTANCE FM	ASSISTANCE FM
300J377920105000	ISACHSEN J-37	3966.1	3975.2	9.1	9.1	0	NANSEN FM	NANSEN FM
300L247930085300	DEPOT PT. L-24	3743.6	3753.3	9.7	9.7	3	VAN HAUEN FM	VAN HAUEN FM
300N277940084300	FOSHEIM N-27	3666.7	3672.5	5.8	4.9	2 to 3	ASSISTANCE FM	ASSISTANCE FM
300N277940084300	FOSHEIM N-27	3943.8	3945.6	1.8	1.3	0	ASSISTANCE FM	ASSISTANCE FM
Total meterage					415			

Table 1. Measured cores and occurrences of shales (modified from Kabanov and Dewing, 2014).

Bulk-element geochemistry

The samples were analyzed at Acme Analytical Laboratories in Vancouver, B.C. with the induced coupled plasma (ICP) instrumentation technique. As indicated above each element in Appendices 1 ([Excel® 2010](#) or [PDF](#) version), 2 ([Excel® 2010](#) or [PDF](#)), and 3 ([composite PDF](#)), samples were run under LF200 (lithogeochemical whole-rock fusion) and AQ200 (geochemical aqua regia digestion) lab codes.

The LF200 code is described as follows. The prepared sample is mixed with LiBO₂/Li₂B₄O₇ flux. Crucibles were fused in a furnace. The cooled bead is dissolved in ACS grade nitric acid and analyzed by ICP and/or ICP-MS. Loss on ignition (LOI) is determined by igniting a sample split then measuring the weight loss.

In the AQ200 code, the prepared sample is digested with a modified Aqua Regia solution of equal parts concentrated HCl, HNO₃ and DIH₂O for one hour in a heating block or hot water bath. The sample then is made up to volume with dilute HCl. Sample splits of 0.5g are analyzed. Optional 15g or 30g digestion are available for AQ200.

In addition, total carbon and total sulphur were measured by Leco combustion (TC000 lab code). In this procedure, the induction flux is added to the prepared sample and then ignited in an induction furnace. A carrier gas sweeps up released carbon to be measured by adsorption in an infrared spectrometric cell. Results are total and attributed to the presence of carbon and sulphur in all forms.

Rock-Eval 6 pyrolysis

The pyrolysis-combustion tests (Appendix 3 ([composite PDF](#))) were conducted using Turbo Rock-Eval 6 device at the Organic Petrology and Geochemistry Laboratory of GSC (Calgary). The pyrograms are archived in Appendix 3 ([composite PDF](#)). The method summary is given after Issler et al. (2012). The test must be an aliquot of a representative amount of rock. The smallest representative amount of sampled rock is roughly estimated in 0.5g or 5 mm³ for hydrocarbon-rich facies (e.g., black shales) and up to 2.5g (1 cm³) for hydrocarbon-lean rocks such as limestones. Approximately 70 milligram samples are initially heated at 300°C for 3 minutes to volatilize any free hydrocarbons (HC) and these are represented by the S1 curve. Ideally, the area under the S1 pyrolysis curve (mg HC/g of initial rock) represents hydrocarbons generated *in situ* over geologic time but sample impregnation by migrated hydrocarbons, expulsion and loss of hydrocarbons or organic drilling contaminants (e.g. oil-based drilling mud) can also affect the results.

Following this isothermal heating step, samples were heated linearly from 300°C to 650°C at 25°C/minute, yielding an S2 curve on pyrograms (Appendix 3 ([composite PDF](#))) that represents thermal cracking of sedimentary organic matter. Under ideal conditions, the area under the S2 curve (mg HC/g of initial rock) represents the remaining potential of the rock sample to generate petroleum from kerogen at increased thermal maturity levels but results can be affected by migrated bitumen and organic drilling contaminants.

The temperature at peak generation on the S2 pyrolysis curve (T_{peak}) is converted to the relative temperature and accepted thermal maturity parameter, T_{max} (in °C), which was established using the older Rock-Eval 2 technology.

The S3 curve corresponds to the amount of CO₂ (mg CO₂/g of initial rock) generated from organic matter during the initial isothermal heating step and the programmed heating phase up to 400°C. CO₂ generated between 400°C and 650°C is from the thermal decomposition of carbonate minerals. The Rock-Eval 6 instrument also records the amount of CO generated during pyrolysis and attributes various proportions to organic carbon and mineral sources, depending on sample temperature. The amount of pyrolysable organic carbon (PC) is determined by combining the S1, S2, S3 and CO contributions according to a specific formula. Pyrolysis mineral carbon is determined from the high temperature portions of the CO and CO₂ pyrolysis curves.

Following pyrolysis, samples are transferred to an oxidation oven where they were linearly heated from 300°C to 850°C to determine the amount of residual organic carbon (RC) and oxidation mineral carbon from CO and CO₂ generated during oxidation. The total organic carbon (TOC in weight %) is the sum of the pyrolysable and residual organic carbon. Similarly, mineral carbon (MINC) is the sum of the pyrolysis and oxidation mineral carbon.

RESULTS ON SHALE SAMPLES

Lithofacies subdivision of shales

Out of 52 measured cores totaling 415 m in thickness, twenty cores contained relatively thick (over 2 m) shales or were entirely composed of shales ([Table 1](#)). Shales were encountered in the Hare Fiord, Belcher Channel, Canyon Fiord, Van Hauen, and Assistance formations. All shales are marine based on trace-fossil and skeletal fossil signatures. All shales except for red-mottled (oxidized) ones contain visually important amount of coaly detritus (Kabanov and Dewing, 2014). Based on lithofacies observations, the shales were classified into three groups: (1) red-mottled; (2) dark low-chroma bioturbated; and (3) dark low-chroma laminated. Otherwise similar and intergrading, groups 2 and 3 are distinguished by the bioturbation index falling below 2 which preserves lamination with rare discrete trace fossils ([Table 2](#); Taylor and Goldring, 1993; Taylor et al., 2003).

Grade	%Bioturbated	Classification
0	0	No bioturbation
1	1-5	Sparse bioturbation: few discrete traces and/or escape structures
2	6-30	Low bioturbation: bedding distinct, low trace density, escape structures often common
3	31-60	Moderate bioturbation: bedding boundaries sharp, traces discrete
4	61-90	High bioturbation: bedding boundaries indistinct, high trace density with overlap common
5	91-99	Intense bioturbation: bedding completely disturbed, limited reworking due to repeated overprinting
6	100	Complete bioturbation: sediment reworking due to repeated overprinting

Table 2. Bioturbation index (BI), based on Taylor & Goldring (1993) and Taylor et al. (2003).

The Group 1 (red-mottled) shales are both bioturbated and laminated shales that were flushed (weathered) by meteoric waters during sea level lowstands ([Figure 3](#)). Vadose weathering is evident from a typical mottled appearance with high-chroma red colors from oxidized iron overprinted by drab-colored grey (reduced iron) mottles ([Figures 3A](#) and [3B](#)). Oxidized shales can be both bioturbated ([Figure 3A](#)) and laminated ([Figure 3B](#)), consistent with deep base level drops caused by high-amplitude sea level fluctuations of the Late Paleozoic ice age (LPIA). In some cases laminated and bioturbated shales are directly involved in paleosol profiles ([Figures 3A](#) and [3B](#)).

The Group 2 (dark bioturbated) shales are fine-grained siliciclastic rocks ranging from true shales to muddy siltstones ([Figure 4](#)). They are typically grey to dark grey, may contain siderite nodules, partly preserve lamination ([Figure 3B](#)), or lack lamination in severely bioturbated varieties ([Figures 4C-E](#)). Bioturbation index is higher than 2 ([Table 2](#)). Mudrocks of the Middle Permian van Hauen Formation are notably enriched in cherty material and grading to chertstones from abundant silicisponge spicules and spicule-derived chalcedony ([Figures 4A, 4B, and 4E](#); Beauchamp and Baud, 2002). Bioturbation patterns are diverse and include trace fossils *Phycosyphon* and/or *Chondrites* ([Figures 4C and 4E](#)), *Zoophycos*, *Planolites*, *Asterosoma*, and *Rosselia* (see core descriptions in Kabanov and Dewing, 2014).

The Group 3 (dark laminated) shales is represented by only 12 samples which are generally finer grained and more pyritic than the shales of Group 2 ([Figures 5A and 5B](#)). Lamination is manifested by pyrite concentrations and slight lithological differences (e.g., discrete laminae enriched in very fine coaly detritus, also known as attritus). The lamination is usually punctuated by discrete trace-fossil clusters with no zero-bioturbated shales encountered. Dark laminated shales are infrequent. Only one 10-m-thick core from the van Hauen Formation (Depot Point L-24 at 3743.6-3753.3 m) consists throughout of Group 3 shales ([Figure 5B](#)). Other occurrences of Group 3 shales show stratigraphic gradation into more

bioturbated shales. The shaly unit of the Belcher Channel Formation cored at 5449-5467 m of Marryatt K-71 well is mostly classified into Group 2 but shows an interval with depressed bioturbation formally included into Group 3 ([Figure 5C](#)). In difference to other Group 3 shales, this interval is less pyritic, contains siderite nodules and impoverished assemblage of benthic macrofossils ([Figures 5C](#) and [5D](#)).

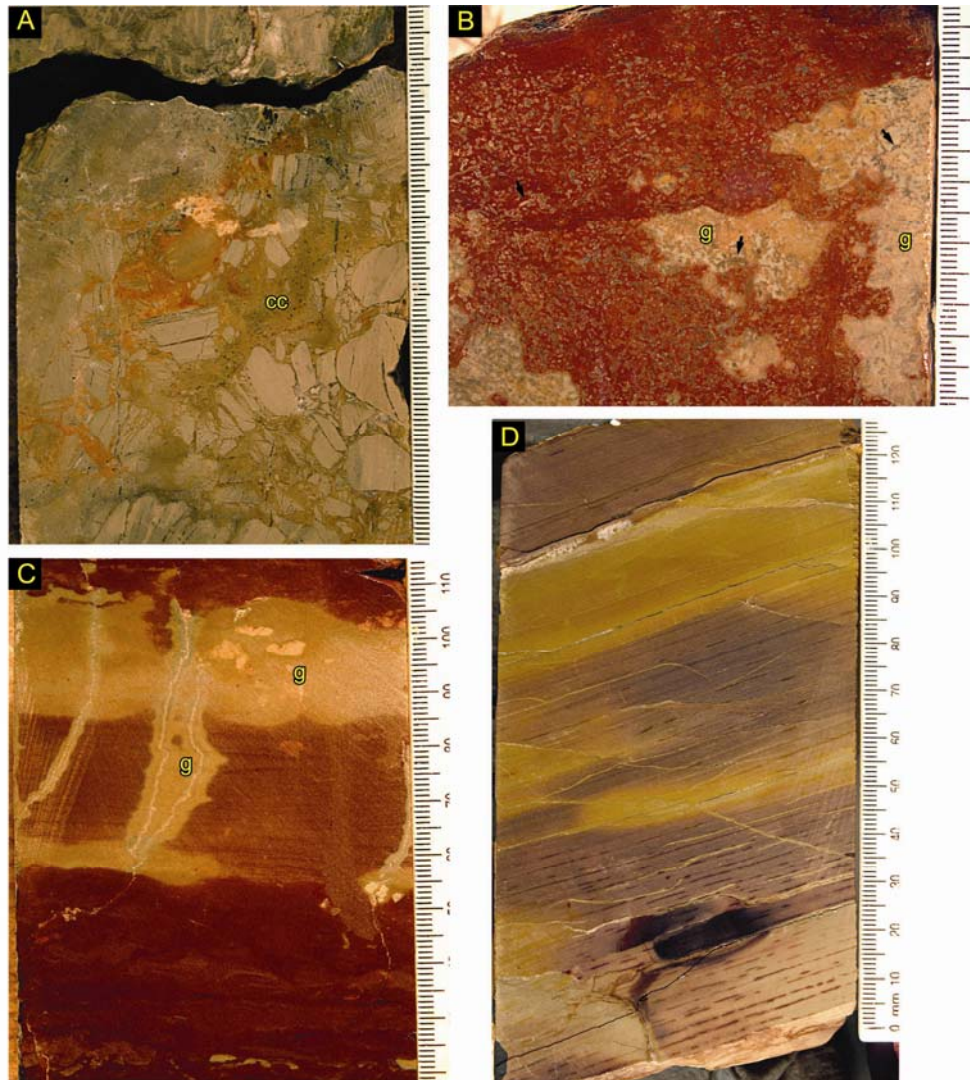


Figure 3. Red-mottled shales of Group 1: (A) Brecciated and calcretized top of a laminated shale unit, (cc) is calcrete deposits between shale clasts; Depot Island C-44, 2460.80-2461.05 m. (B) Red-mottled calcareous mudrock with abundant *Microcodium* (arrowed rods), note gley mottles (g), Jameson Bay C-31, 2406.70 m; (C) Red-mottled partly laminated shale (g - gley mottles and stringers/conduits), Depot Island C-44, 1662-1663 m; (D) Red-mottled laminated shale, same well at 2465.20 m.

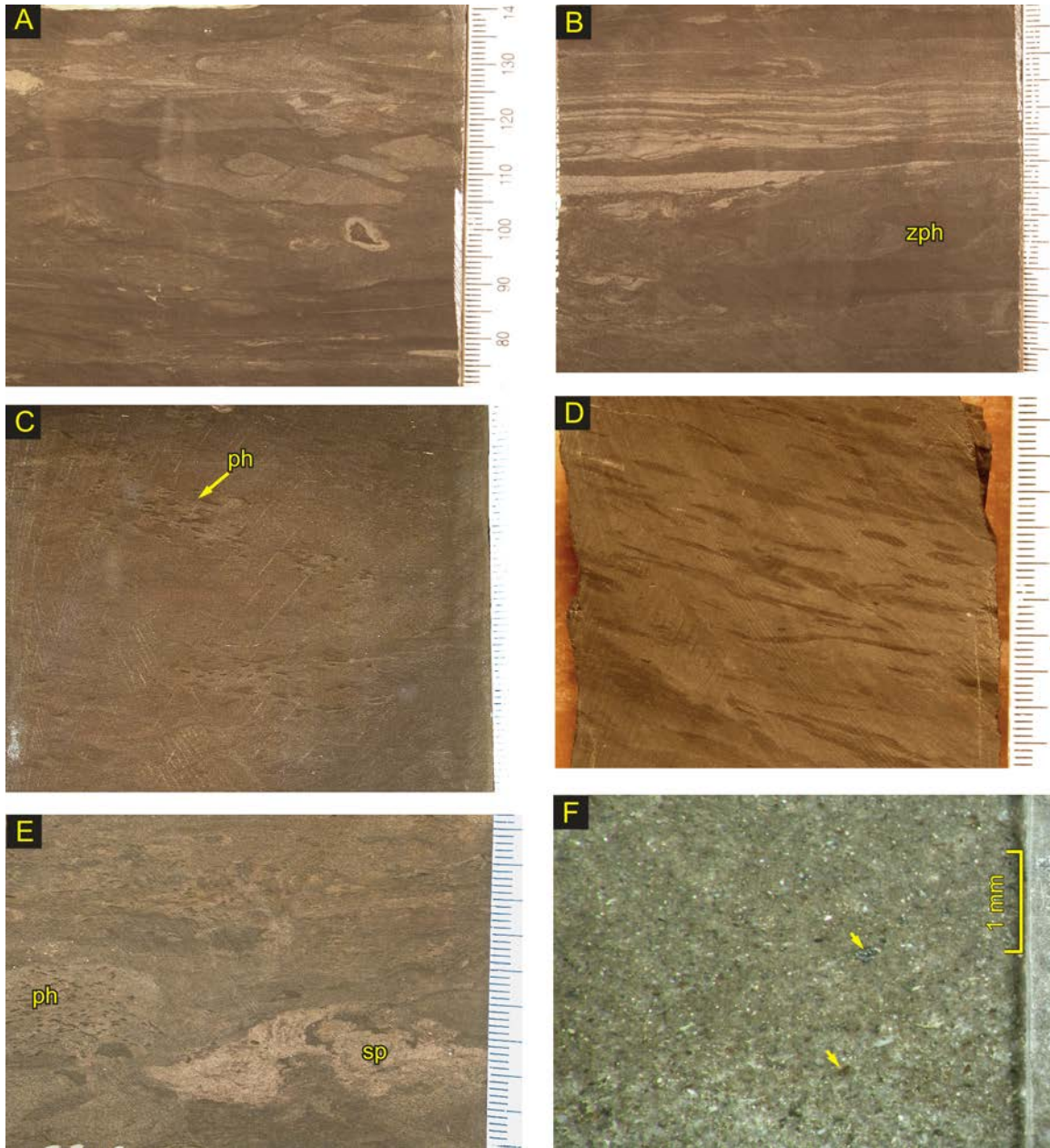


Figure 4. Dark bioturbated shales of Group 2: (A) Calcareous silty mudrock, Brock C-50, 2837.6 m. (B) Calcareous silty mudrock with preserved siltstone laminae, (zph) is *Zoophycos*; Brock C-50, 2839.3 m. (C) Monotonous silty shale with moderate bioturbation (BI3), (ph) are *Phycosyphon* clusters, Drake Point L-67, 3134.4 m. (D) Bioturbated fissile marl, Chads Creek B-64, 5023.5 m. (E) Argillaceous chertstone, (sp) is a collapsed silicisponge (spicule mesh) churned up by burrowing, Drake Point L-67, 3136.5 m. (F) Binocular microphoto of a muddy and sandy siltstone with coal particles (arrowed), Brock C-50, 2841.30 m.

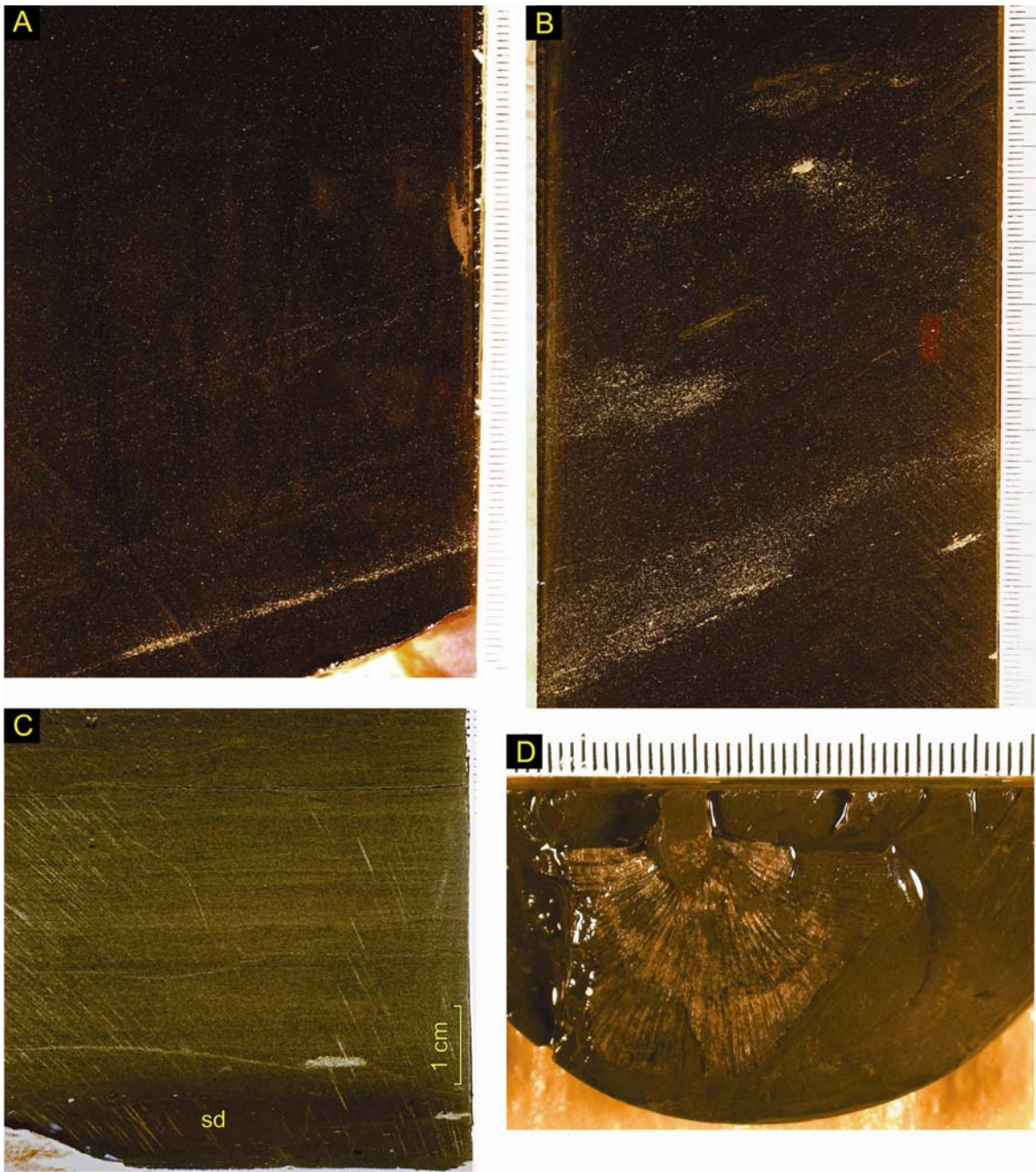


Figure 5. Dark laminated shales of Group 3: (A) Black laminated pyritic shale from interval where TOC exceeds 1%, Fosheim N-27, 3667.15 m. (B) Homogeneous cryptolaminated pyritic mudrock, Depot Point L-24, 3746.03-3746.46. (C, D) Dark laminated shale with calcisiltite laminae, Marryatt K-71, 5450.65 m; (D) an orthotetrid brachiopod on lamination plane.

Properties of organic matter based on Rock-Eval pyrolysis

Rock-Eval pyrolysis/TOC results for the 90 samples are given in Appendix 3 ([composite PDF](#)). Total organic carbon content (TOC wt%) are low, with an average TOC of 0.63% and a maximum value of 1.84% ([Figure 6](#); n=90). 59 of the 90 samples have TOC less than 0.50%. Highest TOC values are from Fosheim N-27 well at about 3670 m.

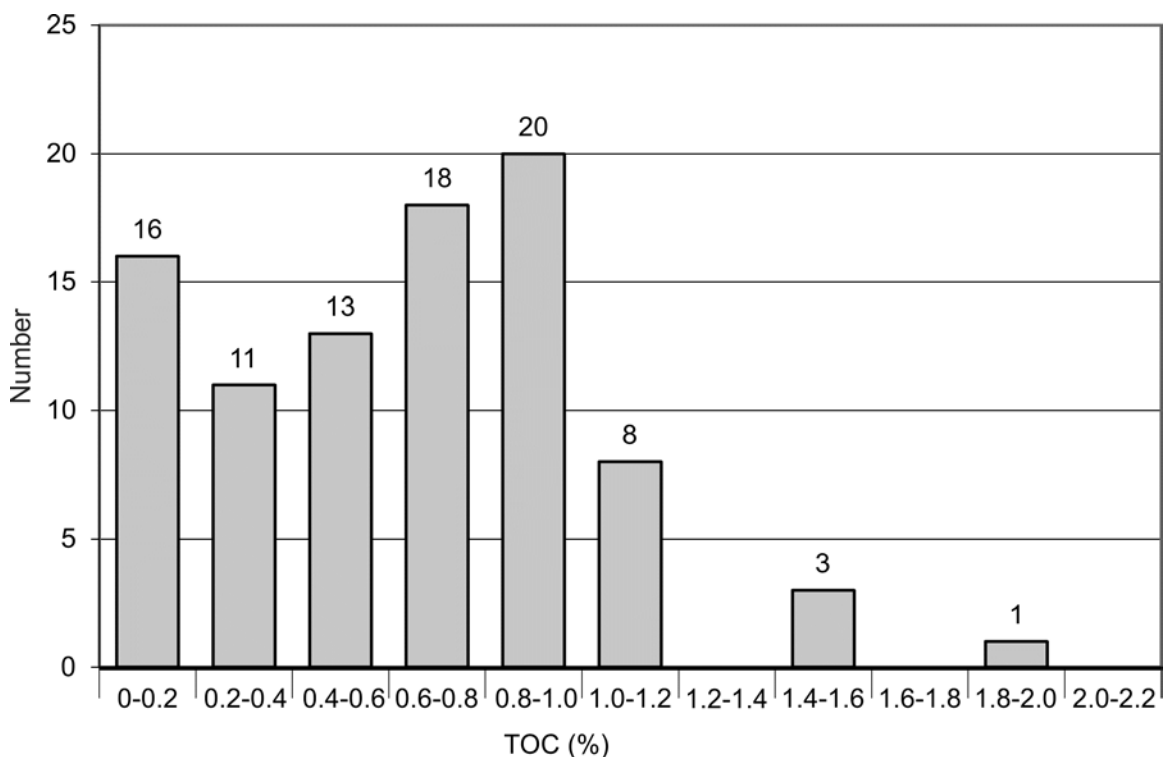


Figure 6. Histogram of Total Organic Carbon (%) from this study.

Hydrogen Index (HI; $100 \times S_2/TOC$) averages 58 mg HC/g TOC (n = 90). Higher HI values are generally in samples with very low TOC (<0.2%) so the significance of the values to hydrocarbon prospectivity are suspect. HI values of greater than 100 are present in Drake Point L-67 (3135 to 3139 m and 3238 to 3251 m; van Hauen Formation) in samples with TOC ranging between 0.48% and 0.83%.

Kerogen type can be estimated from S_2 vs TOC and pseudo-van Krevelen diagrams ([Figure 7](#)). Most samples from this study fall on the Type III kerogen line, except for those samples from Drake Point L-67 (van Hauen Formation) and possibly one low TOC sample from Jameson Bay C-31 (Canyon Fiord Formation). These samples are more typical of Type II kerogen types.

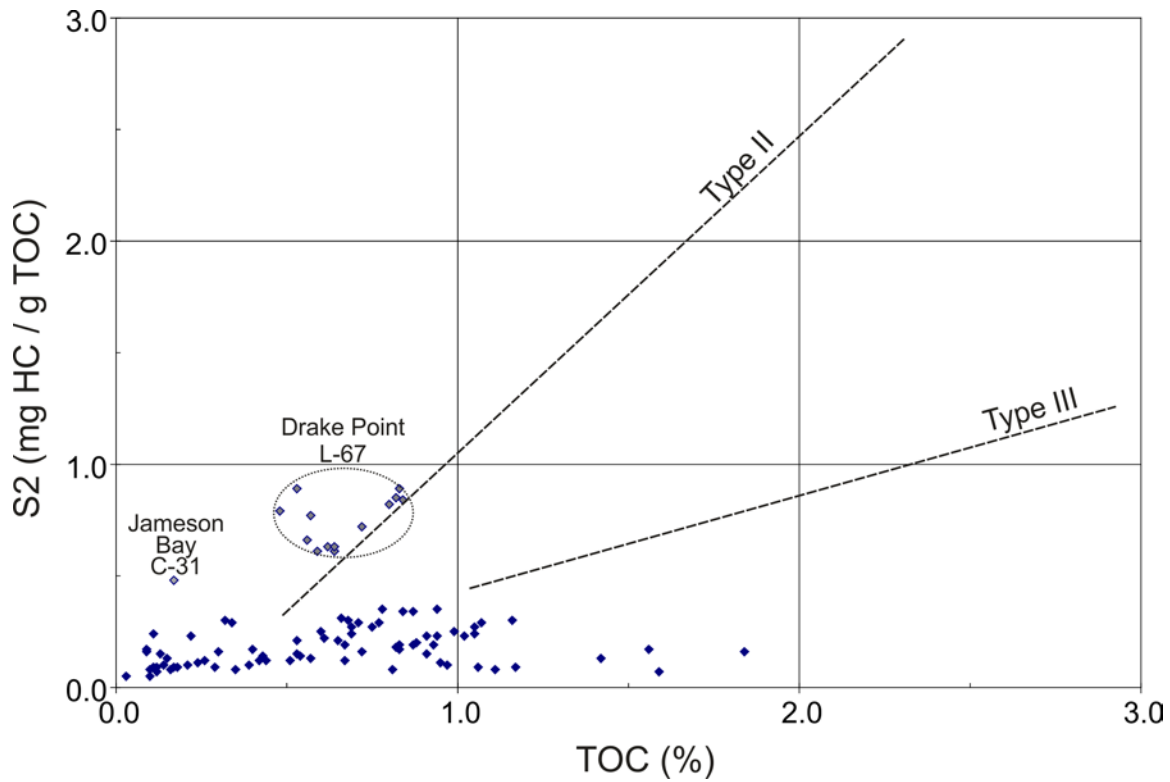


Figure 7. S2 vs TOC showing samples from this study. Type II curve based on well characterized lower Paleozoic Cape Phillips Formation samples in Obermajer et al. (2007). Samples from Drake Point L-67 and one sample from Jameson Bay C-31 plot closer to a typical Type II kerogen.

Samples from this study (black dots on [Figure 8](#)) are compared to all other samples from the upper Paleozoic of the Arctic (green dots; Obermajer et al., 2007) on a pseudo-van Krevelen diagram. Samples in this data set fall on the Type III curve, with the exception of samples from Drake Point L-67 that fall on the typical Type II curve.

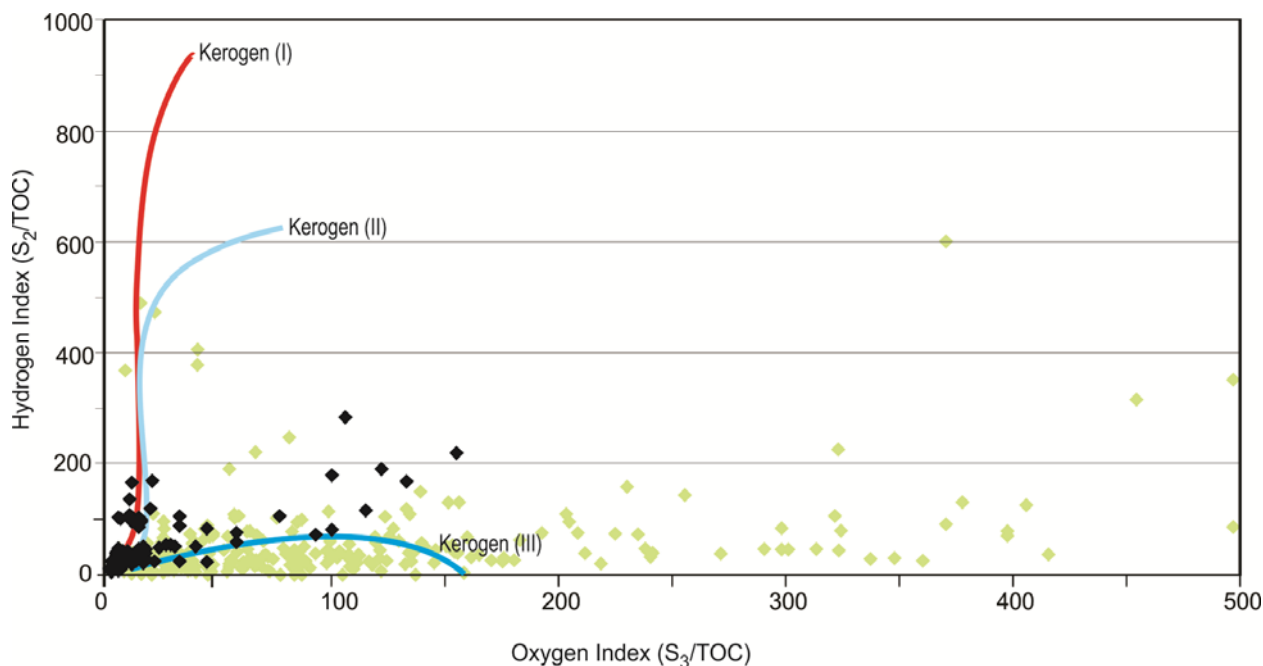


Figure 8. Pseudo- van Krevelen diagram showing HI vs. OI. Most samples from this study (black) are typical Type III kerogen, except those from Drake Point L-67. All other upper Paleozoic samples from Obermajer et al. (2007) shown in green for comparison.

Tmax values, which are considered reliable for samples with TOC greater than 0.5% and S2 greater than 0.2 mgHC/g rock (Peters, 1986), range from 432°C to 561°C (Appendices 2 ([Excel® 2010](#) or [PDF](#)), and 3 ([composite PDF](#))). [Table 3](#) compares Tmax values from core (this study) with Tmax values from cuttings at approximately the same depth (Obermajer et al. 2007). In most cases, samples from core and cuttings return similar Tmax values.

Well name	Depth	Core/cuttings	Tmax	Reference
Robert Harbour K-07	2606.04	cuttings	431	Obermajer et al. 2007
Robert Harbour K-07	2714.0	core	433	This report
Robert Harbour K-07	2715.1	Core	433	This report
Robert Harbour K-07	2716.3	Core	434	This report
Robert Harbour K-07	2717.4	Core	432	This report
Robert Harbour K-07	2718.4	Core	433	This report
Robert Harbour K-07	2719.5	Core	434	This report
Robert Harbour K-07	2720.5	Core	436	This report
Robert Harbour K-07	2721.4	Core	432	This report
Robert Harbour K-07	2849.88	Cuttings	434	Obermajer et al. 2007
DRAKE POINT L-67	3137.5	Core	441	This report
DRAKE POINT L-67	3139.3	Core	438	This report
DRAKE POINT L-67	3234.7	Core	441	This report
DRAKE POINT L-67	3236.5	Core	441	This report
DRAKE POINT L-67	3238.3	Core	442	This report
DRAKE POINT L-67	3239.9	Core	442	This report
DRAKE POINT L-67	3242.0	Core	443	This report

DRAKE POINT L-67	3243.4	Core	441	This report
DRAKE POINT L-67	3245.2	Core	443	This report
DRAKE POINT L-67	3247.6	Core	442	This report
DRAKE POINT L-67	3249.2	Core	442	This report
DRAKE POINT L-67	3251.2	Core	441	This report
DRAKE POINT L-67	3252	Core	447	Obermajer et al. 2007
SATELLITE F-68	2633.5	Cuttings	418	Obermajer et al. 2007
SATELLITE F-68	2651.8	Cuttings	456	Obermajer et al. 2007
SATELLITE F-68	2664.2	Core	462	This report
SATELLITE F-68	2664.8	Core	463	This report
SATELLITE F-68	2665.7	Core	466	This report
SATELLITE F-68	2666.1	Core	468	This report
SATELLITE F-68	2667.2	Core	468	This report
SATELLITE F-68	2668.1	Core	460	This report
SATELLITE F-68	2668.7	Core	459	This report
SATELLITE F-68	2673.1	Cuttings	393	Obermajer et al. 2007
SATELLITE F-68	2688.3	Cuttings	457	Obermajer et al. 2007
SATELLITE F-68	3173.0	Cuttings	497	Obermajer et al. 2007
SATELLITE F-68	3186.2	Core	504	This report
SATELLITE F-68	3187.3	Core	498	This report
SATELLITE F-68	3188.1	Core	509	This report
SATELLITE F-68	3189.1	Core	512	This report
SATELLITE F-68	3190.2	Core	515	This report
SATELLITE F-68	3191.2	Core	515	This report
SATELLITE F-68	3192.0	Cuttings	503	Obermajer et al. 2007
SATELLITE F-68	3192.0	Core	510	This report
SATELLITE F-68	3200.4	Cuttings	455	Obermajer et al. 2007
SATELLITE F-68	3200.4	Cuttings	506	Obermajer et al. 2007

Table 3. Tmax values from core (this study) vs. cuttings (Obermajer et al. 2007) at approximately the same depth.

Geochemical results

Proxies based on elemental composition and TOC of shales are widely used to reconstruct sediment sourcing and redox/anoxia depositional conditions (Calvert and Pedersen, 1993; Algeo and Maynard, 2008). In analyzed shale samples, the highest TOC values are reached in Group 3 (up to 1.84%; Figure 9). Red-mottled shales are lean in TOC (up to 0.39%) with the highest scatter of TOC values expressed in high positive skewness on [Figure 9](#) ($\gamma=1.74$). This confirms that the connate organic matter has been lost during vadose oxidation.

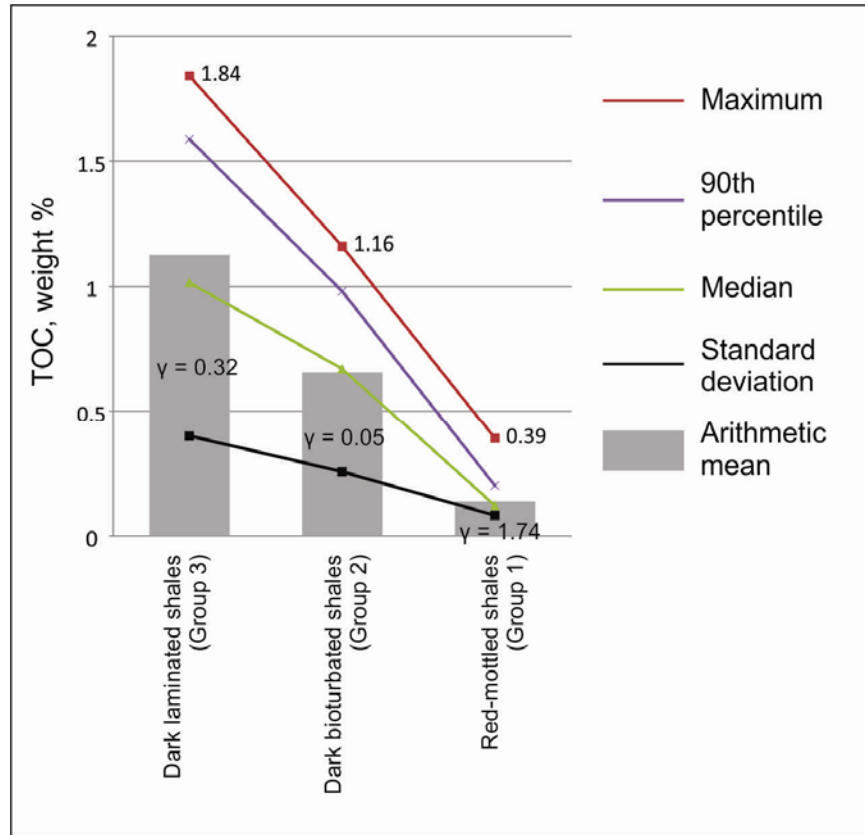


Figure 9. TOC in three groups of shales. Skewness (γ) is given in numbers.

Rare and trace metals that are known to precipitate across redox barrier (Mn) and in anoxic environments (Mo, Pb, U, V, Cu, Ni, Zn) are normalized to alumina for analysis, which is a common practice to reduce detrital input of these metals bound in aluminosilicates (Calvert and Pedersen, 1993; Algeo and Maynard, 2008). Pearson r correlation of TOC and Me/Al ([Figure 10](#)) shows essential lack of correlation between Pb, U, V, Ni and the organic matter content.

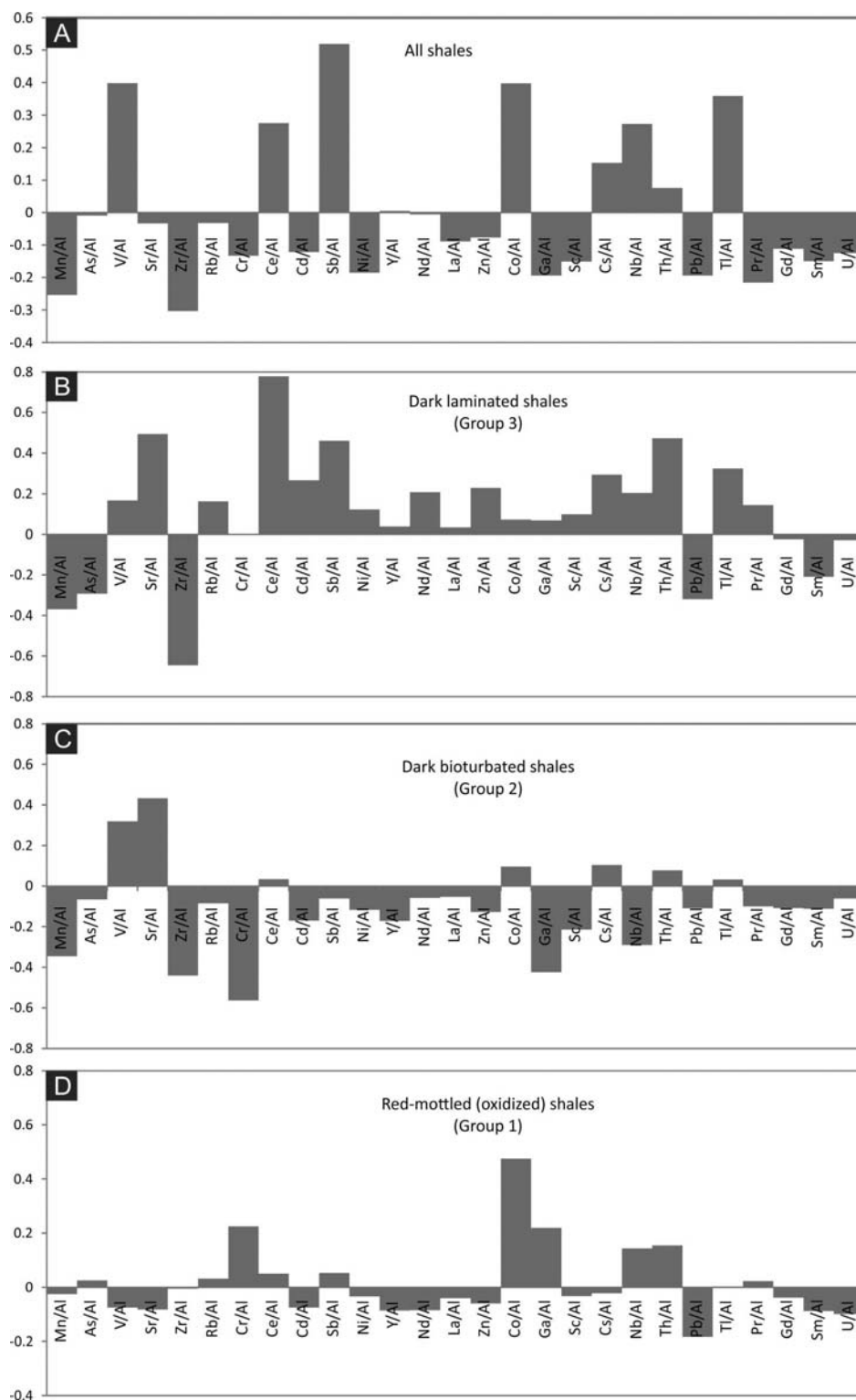


Figure 10. Pearson r correlation of TOC and Al-normalized metals in all shale samples (A), Group 3 (B), Group 2 (C), and Group 1 (D).

Correlation tables of elements in dark laminated and bioturbated shales (Tables 3, 4, and 5) shows lack or insufficient positive covariation between U, Pb, V, and Ni. Molybdenum and copper were essentially lacking in analyzed shale samples (maximum values below 10 ppm) and are excluded from analysis. Manganese is expected to show negative covariation with anoxia-sensitive metals in response to fluctuation between redox and anoxic facies in a stratigraphic column. This pattern is also absent with values fluctuating between weakly negative to weakly positive (Tables 3, 4, and 5). This suggests that permanent anoxic sulphidic conditions weren't reached even in Group 3 laminated shales.

	Mn	As	V	Sr	Zr	Rb	Cr	Ce	Cd	Sb	Ni	Y	Nd	La	Zn	Co	Ga	Sc	Cs	Nb	Th	Pb	Tl	Pr	Gd	Sm	U
Mn	1																										
As	0.46	1																									
V	-0	0.27	1																								
Sr	-0	0.18	0.07	1																							
Zr	0.77	0.24	-0.1	0.05	1																						
Rb	0.39	0.52	0.23	0.09	0.2	1																					
Cr	0.34	0.22	0.02	0.06	0.19	0.12	1																				
Ce	0.1	0.72	0.39	0.13	-0.1	0.66	0.14	1																			
Cd	0.61	0.31	-0	-0.2	0.41	0.45	0.06	0.23	1																		
Sb	0.16	0.47	0.44	-0.1	0	0.32	0.34	0.64	0.12	1																	
Ni	0.55	0.28	0.06	-0.1	0.42	0.29	0.08	0	0.24	0.13	1																
Y	0.18	0.05	0.14	0.38	0.19	0.34	0.24	0.16	-0	0.24	0.21	1															
Nd	0.55	0.69	0.26	0.19	0.23	0.65	0.16	0.66	0.71	0.46	0.25	0.16	1														
La	0.54	0.56	0.1	-0	0.25	0.59	0.09	0.5	0.9	0.25	0.24	-0	0.88	1													
Zn	0.56	0.62	0.11	-0	0.32	0.67	0.12	0.6	0.88	0.32	0.23	0.03	0.85	0.95	1												
Co	0.08	0.21	0.18	0.02	-0	0.16	0.05	0.24	0.05	0.58	0.21	0.11	0.2	0.1	0.12	1											
Ga	0.81	0.29	0.03	-0.2	0.64	0.15	0.44	-0.1	0.46	0.3	0.63	0.11	0.34	0.34	0.36	0.21	1										
Sc	-0.1	0.1	-0.1	0.26	-0.2	0.17	0.44	0.23	-0.2	0.03	-0.1	0.14	0.02	-0	0.01	-0.1	-0.1	1									
Cs	0.24	0.13	0.15	-0.3	0.01	0.07	-0.1	0.15	0.61	0.32	0.17	-0.2	0.5	0.57	0.46	0.22	0.28	-0.3	1								
Nb	0.25	0.01	0.17	-0.1	0.13	0.18	0.6	0.15	0.09	0.44	0.08	0.14	0.14	0.02	0.07	0.16	0.39	0.16	0.09	1							
Th	0.19	0.5	0.23	0.18	0.06	0.84	0.16	0.7	0.31	0.35	0.18	0.23	0.58	0.5	0.61	0.17	0.03	0.3	-0	0.24	1						
Pb	0.42	0.37	0.07	0.04	0.27	0.78	0.05	0.41	0.66	0.05	0.24	0.2	0.66	0.71	0.72	-0	0.16	0.07	0.25	0.08	0.62	1					
Tl	0.08	0.35	0.47	0.06	-0	0.43	0.05	0.6	0.1	0.64	0.11	0.6	0.4	0.23	0.31	0.37	0.05	0.03	0.17	0.13	0.42	0.21	1				
Pr	0.27	0.39	0.01	0.33	0.05	0.43	0.1	0.37	0.32	-0	0.04	0.13	0.39	0.43	0.47	-0	0.05	0.34	0.05	-0.1	0.37	0.4	0.15	1			
Gd	0.53	0.55	0.08	-0.1	0.25	0.63	0.09	0.51	0.9	0.24	0.27	0.01	0.84	0.97	0.95	0.12	0.34	-0	0.54	-0	0.51	0.73	0.24	0.44	1		
Sm	0.66	0.61	0.16	0.08	0.35	0.53	0.12	0.42	0.83	0.27	0.33	0.04	0.93	0.92	0.84	0.12	0.45	-0.1	0.59	0.07	0.4	0.67	0.22	0.37	0.88	1	
U	0.6	0.5	0.08	0.05	0.32	0.52	0.13	0.39	0.87	0.2	0.22	0.03	0.89	0.93	0.85	0.07	0.37	-0.1	0.57	0.08	0.42	0.68	0.17	0.37	0.9	0.96	1

Table 4. Pearson r correlation matrix of trace metals in all shale samples from studied cores (only for elements with maximum values exceeding 10 ppm).

	Mn	As	V	Sr	Zr	Rb	Cr	Ce	Cd	Sb	Ni	Y	Nd	La	Zn	Co	Ga	Sc	Cs	Nb	Th	Pb	Tl	Pr	Gd	Sm	U
Mn	1																										
As	0.516	1																									
V	0.079	0.535	1																								
Sr	-0.1	0.345	0.496	1																							
Zr	0.789	0.183	-0.1	-0.06	1																						
Rb	0.434	0.666	0.644	0.394	0.246	1																					
Cr	0.419	0.227	-0.19	-0.54	0.249	0.172	1																				
Ce	0.134	0.781	0.67	0.546	-0.13	0.735	0.102	1																			
Cd	0.747	0.623	0.22	0.205	0.549	0.69	0.43	0.442	1																		
Sb	0.408	0.708	0.506	0.304	0.147	0.573	0.387	0.737	0.537	1																	
Ni	0.853	0.425	0.235	0.104	0.712	0.475	0.178	0.117	0.617	0.351	1																
Y	0.269	0.09	0.219	-0.15	0.324	0.4	0.167	0.143	0.195	0.236	0.435	1															
Nd	0.568	0.886	0.61	0.413	0.259	0.768	0.263	0.803	0.763	0.769	0.466	0.105	1														
La	0.545	0.825	0.451	0.387	0.267	0.77	0.308	0.749	0.861	0.677	0.437	0.103	0.923	1													
Zn	0.562	0.808	0.441	0.415	0.306	0.828	0.336	0.779	0.878	0.701	0.474	0.177	0.907	0.95	1												
Co	0.311	0.26	0.273	0.275	0.05	0.334	-0.06	0.202	0.326	0.264	0.35	-0.04	0.323	0.32	0.29	1											
Ga	0.872	0.317	-0.15	-0.23	0.718	0.187	0.543	-0.06	0.592	0.382	0.774	0.237	0.351	0.334	0.376	0.225	1										
Sc	-0.1	0.177	-0.05	-0.05	-0.21	0.241	0.405	0.349	0.108	0.244	-0.22	-0.02	0.151	0.251	0.311	-0.07	-0.04	1									
Cs	0.31	0.549	0.307	0.319	0.126	0.25	-0.02	0.406	0.324	0.444	0.271	-0.2	0.526	0.434	0.377	0.4	0.193	-0.21	1								
Nb	0.441	0.151	-0.09	-0.09	0.34	0.165	0.672	-0.453	0.304	0.402	0.018	0.247	0.257	0.316	0.145	0.63	0.2	0.08	1								
Th	0.207	0.566	0.599	0.526	0.061	0.852	0.167	0.739	0.579	0.592	0.253	0.241	0.723	0.726	0.783	0.304	0.06	0.353	0.234	0.291	1						
Pb	0.417	-0.58	0.518	0.335	0.315	0.877	0.231	0.612	0.695	0.451	0.441	0.328	0.685	0.728	0.773	0.286	0.192	0.257	0.238	0.256	0.775	1					
Tl	0.199	0.495	0.621	0.338	0.059	0.709	-0.01	0.676	0.316	0.532	0.379	0.681	0.522	0.476	0.538	0.317	0.034	0.183	0.129	-0.04	0.633	0.578	1				
Pr	0.247	0.622	0.302	0.371	0.001	0.541	0.133	0.622	0.439	0.469	0.223	0.046	0.486	0.557	0.591	0.397	0.143	0.419	0.291	0.075	0.419	0.493	0.451	1			
Gd	0.541	0.798	0.43	0.348	0.273	0.805	0.322	0.749	0.883	0.636	0.429	0.176	0.897	0.965	0.959	0.287	0.318	0.264	0.374	0.227	0.719	0.759	0.513	0.586	1		
Sm	0.704	0.848	0.492	0.287	0.402	0.708	0.296	0.632	0.846	0.666	0.574	0.082	0.943	0.92	0.868	0.377	0.475	0.048	0.54	0.274	0.589	0.673	0.404	0.452	0.889	1	
U	0.642	0.778	0.44	0.268	0.375	0.693	0.342	0.6	0.858	0.604	0.474	0.077	0.906	0.92	0.859	0.318	0.42	0.083	0.462	0.3	0.63	0.654	0.364	0.419	0.905	0.953	1

Table 5. Pearson r correlation matrix of trace metals in Group 2 shales (only for elements with maximum values exceeding 10 ppm).

	Mn	As	V	Sr	Zr	Rb	Cr	Ce	Cd	Sb	Ni	Y	Nd	La	Zn	Co	Ga	Sc	Cs	Nb	Th	Pb	Tl	Pr	Gd	Sm	U
Mn	1																										
As	-0.14	1																									
V	-0.26	-0.04	1																								
Sr	-0.63	-0.07	0.159	1																							
Zr	0.736	0.422	-0.27	-0.82	1																						
Rb	0.037	-0.65	-0.16	0.463	-0.53	1																					
Cr	0.493	-0.59	0.037	-0.49	0.201	0.113	1																				
Ce	-0.43	-0.37	-0.02	0.72	-0.83	0.607	-0.04	1																			
Cd	0.171	0.105	-0.55	0.295	0.007	0.351	-0.38	0.308	1																		
Sb	-0.73	0.118	0.141	0.781	-0.76	0.306	-0.6	0.694	0.267	1																	
Ni	-0.11	-0.08	0.484	-0.22	-0.01	-0.43	0.314	-0.14	-0.56	-0.06	1																
Y	-0.58	0.021	-0	0.699	-0.58	0.382	-0.31	0.476	0.115	0.701	0.11	1															
Nd	-0.47	0.119	-0.07	0.691	-0.58	0.528	-0.57	0.615	0.411	0.884	-0.4	0.643	1														
La	0.228	0.483	-0.45	0.145	0.239	0.137	-0.45	0.128	0.839	0.172	-0.55	0.049	0.367	1													
Zn	-0.03	0.276	-0.35	0.545	-0.14	0.378	-0.51	0.406	0.854	0.378	-0.63	0.295	0.525	0.886	1												
Co	-0.21	0.286	-0.15	0.469	-0.23	0.28	-0.73	0.234	0.636	0.58	-0.32	0.419	0.638	0.65	0.677	1											
Ga	-0.27	0.296	0.699	-0.01	-0.05	-0.42	-0.2	-0.15	-0.25	0.311	0.67	0.162	0.047	-0.17	-0.27	0.194	1										
Sc	0.596	-0.24	-0.28	-0.44	0.339	0.017	0.542	-0.01	0.25	-0.34	0.11	-0.32	-0.29	0.147	-0.07	-0.01	-0.01	1									
Cs	-0.55	-0.12	0.206	0.365	-0.58	0.152	-0.27	0.37	-0.1	0.743	0.391	0.596	0.589	-0.29	-0.21	0.336	0.531	-0.07	1								
Nb	0.053	-0.93	0.088	0.053	-0.46	0.664	0.638	0.401	-0.26	-0.03	0.061	0.067	0.018	-0.56	-0.38	-0.36	-0.26	0.201	0.227	1							
Th	-0.09	-0.67	-0.16	0.605	-0.65	0.864	-0.04	0.68	0.396	0.324	-0.42	0.249	0.406	0.098	0.423	0.272	-0.49	-0.1	0.077	0.558	1						
Pb	0.44	-0.35	-0.3	-0.07	0.086	0.699	0.236	0.075	0.191	-0.21	-0.36	0.094	0.12	0.276	0.277	0.081	-0.52	-0.02	-0.3	0.352	0.473	1					
Tl	-0.75	0.314	0.264	0.721	-0.55	-0.13	-0.54	0.381	0.032	0.765	0.233	0.706	0.515	-0.05	0.183	0.267	0.426	-0.47	0.59	-0.27	-0.02	-0.54	1				
Pr	-0.01	0.164	0.042	0.079	0.032	-0.08	-0.2	-0.03	0.15	-0.09	-0.64	-0.47	0.02	0.187	0.235	0.103	-0.24	0.037	-0.41	-0.16	0.061	-0.26	-0.19	1			
Gd	0.134	0.296	-0.41	0.231	0.118	0.304	-0.44	0.116	0.819	0.117	-0.64	0.096	0.319	0.911	0.906	0.667	-0.27	0.022	-0.37	-0.41	0.28	0.402	-0.12	0.262	1		
Sm	-0.15	0.351	-0.07	0.101	-0.03	0.033	-0.54	-0.01	0.153	0.508	-0.29	0.156	0.673	0.174	0.063	0.437	0.217	-0.12	0.535	-0.18	-0.12	-0.15	0.255	0.14	0	1	
U	-0.07	0.23	-0.5	0.202	-0.14	0.348	-0.27	0.483	0.574	0.454	-0.54	0.218	0.654	0.669	0.586	0.562	-0.24	0.271	0.14	-0.11	0.195	0.206	-0.02	0.219	0.549	0.449	1

Table 6. Pearson r correlation matrix of trace metals in Group 3 shales (only for elements with maximum values exceeding 10 ppm).

ACKNOWLEDGEMENTS

This work is a contribution to the Sverdrup Basin (ARC003) activity of the Western Arctic Project of the [Geomapping for Energy and Minerals \(GEM-2\) Programme](#). The authors are thankful to Steve Grasby (GSC) for critical review, Damien Weleschuk ([U of C](#) – GSC) for assistance with sampling, and Richard Fontaine and William Dwyer of the [NEB Core and Sample Repository](#) at [GSC-Calgary](#) for their help with core displays. David Sargent (GSC) is cordially thanked for work on the publication layout. Core samples have been loaned for destructive examination under NEB Sampling Permission 12609 from June 2014.

REFERENCES

- Algeo, J.T. and Maynard, J.B., 2008. Trace-metal covariation as a guide to water-mass conditions in ancient anoxic marine environments; *Geosphere*, v. 4, p. 872-887.
- Beauchamp, B. and Baud, A., 2002. Growth and demise of Permian biogenic chert along northwest Pangea: evidence for end-Permian collapse of thermohaline circulation; *Palaeogeography, Palaeoclimatology, Palaeoecology*, v. 184, pp. 37-63
- Calvert, S.E. and Pedersen, T.F., 1993. Geochemistry of recent oxic and anoxic marine sediments: implications for the geological record; *Marine Geology*, v. 113, p. 67-88.
- Dewing, K. and Embry, A.F., 2007. Geological and Geochemical Data from the Canadian Arctic Islands. Part I: Stratigraphic Tops from Arctic Islands' Oil and Gas Exploration Boreholes; Geological Survey of Canada, Open File Report 5442, 1 CD-ROM.
- Issler, D.R., Obermajer, M., Reyes, J. and Li, M., 2012. Integrated analysis of vitrinite reflectance, Rock-Eval 6, gas chromatography, and gas chromatography-mass spectrometry data for the Mallik A-06, Parsons N-10 and Kugaluk N-02 wells, Beaufort-Mackenzie Basin, northern Canada; Geological Survey of Canada, Open File 6978, 78 p. doi:10.4095/289672
- Kabanov, P.B. and Dewing, K.E., 2014. Geological and geochemical data from the Canadian Arctic Islands. Part XII: Descriptions and lithologs of Upper Paleozoic core; Geological Survey of Canada Open File 7569.
- Obermajer, M., Stewart, K. R., and Dewing, K., 2007. Geological and geochemical data from the Canadian Arctic Islands Part II: Rock-Eval/TOC data; Geological Survey of Canada, Open File 5459, CD-ROM.
- Peters, K.E., 1986. Guidelines for evaluating petroleum source rock using programmed pyrolysis; *American Association of Petroleum Geologists, Bulletin* 70, 318-320.
- Taylor, A.M. and Goldring, R., 1993. Description and analysis of bioturbation and ichnofabric; *Journal of the Geological Society (London)*, 150: 141-148.
- Taylor, A.M., Goldring, R., and Gowland, S., 2003. Analysis and application of ichnofabrics; *Earth-Science Reviews*, 60: 227-259.

LIST OF TABLES

- [Table 1.](#) Measured cores and occurrences of shales (modified from Kabanov and Dewing, 2014).
[Table 2.](#) Bioturbation index (BI), based on Taylor & Goldring (1993) and Taylor et al. (2003).
[Table 3.](#) Tmax values from core (this study) vs. cuttings (Obermajer et al. 2007) at approximately the same depth.
[Table 4.](#) Pearson r correlation matrix of trace metals in all analyzed shales (only for elements with maximum values exceeding 10 ppm).
[Table 5.](#) Pearson r correlation matrix of trace metals in Group 3 shales (only for elements with maximum values exceeding 10 ppm).
[Table 6.](#) Pearson r correlation matrix of trace metals in Group 3 shales (only for elements with maximum values exceeding 10 ppm).

LIST OF FIGURES

- [Figure 1.](#) Locations of wells with upper Paleozoic core.
[Figure 2.](#) Stratigraphic nomenclature for the upper Paleozoic of the Canadian Arctic Islands (updated from Dewing and Embry, 2007).
[Figure 3.](#) Red-mottled shales of Group 1: (A) Brecciated and calcretized top of a laminated shale unit, (cc) is calcrete deposits between shale clasts; Depot Island C-44, 2460.80-2461.05 m. (B) Red-mottled calcareous mudrock with abundant *Microcodium* (arrowed rods), note gley mottles (g), Jameson Bay C-31, 2406.70 m. (C) Red-mottled partly laminated shale (g - gley mottles and stringers/conduits), Depot Island C-44, 1662-1663 m. (D) Red-mottled laminated shale, same well at 2465.20 m.
[Figure 4.](#) Dark bioturbated shales of Group 2: (A) Calcareous silty mudrock, Brock C-50, 2837.6 m. (B) Calcareous silty mudrock with preserved siltstone laminae, (zph) is *Zoophycos*; Brock C-50, 2839.3 m. (C) Monotonous silty shale with moderate bioturbation (BI3), (ph) are *Phycosyphon* clusters, Drake Point L-67, 3134.4 m. (D) Bioturbated fissile marl, Chads Creek B-64, 5023.5 m. (E) Argillaceous chertstone, (sp) is a collapsed silicisponge (spicule mesh) churned up by burrowing, Drake Point L-67, 3136.5 m (F) Binocular microphoto of a muddy and sandy siltstone with coal particles (arrowed), Brock C-50, 2841.30 m.
[Figure 5.](#) Dark laminated shales of Group 3: (A) Black laminated pyritic shale from interval where TOC exceeds 1%, Fosheim N-27, 3667.15 m. (B) Homogeneous cryptolaminated pyritic mudrock, Depot Point L-24, 3746.03-3746.46. (C, D) Dark laminated shale with calcisiltite laminae, Marryatt K-71, 5450.65 m; (D) an orthotetid brachiopod on lamination plane.
[Figure 6.](#) Histogram of Total Organic Carbon (%) from this study.
[Figure 7.](#) S2 vs TOC showing samples from this study. Type II curve based on well characterized lower Paleozoic Cape Phillips Formation samples in Obermajer et al. (2007). Samples from Drake Point L-67 and one sample from Jameson Bay C-31 plot closer to a typical Type II kerogen.
[Figure 8.](#) Pseudo- van Krevelen diagram showing HI vs. OI. Most samples from this study (black) are typical Type III kerogen, except those from Drake Point L-67. All other upper Paleozoic samples from Obermajer et al. (2007) shown in green for comparison.
[Figure 9.](#) TOC in three groups of shales. Skewness (γ) is given is numbers.
[Figure 10.](#) Pearson r correlation of TOC and Al-normalized metals in all shale samples (A), Group 3 (B), Group 2 (C), and Group 1 (D).

LIST OF APPENDICES

All appendices are located in the “of7848\appendix” directory of this report.

Appendix 1. ICP-MS/ES geochemical data. The data is available as either a Microsoft® Office Excel® 2010 file ([appendix_1_ICP_data_Acme.xlsx](#)) or as an Adobe® PDF file ([appendix_1_ICP_data_Acme.pdf](#)).

Appendix 2. Rock-Eval 6 data (Excel® 2010 file ([appendix_2_Rock-Eval_results.xls](#)), or Adobe® PDF version ([appendix_2_Rock-Eval_results.pdf](#)).

Appendix 3. Rock-Eval 6 pyrograms (archived). Rock-Eval results compiled in Appendix 3 are available as a composite PDF file ([appendix_3_000_Rock-Eval_6_pyrograms_composite.pdf](#)) or by individual analysis as a separate PDF file as listed below.

1. [01-9107](#)
2. [02-5449.5](#)
3. [02-8755.5](#)
4. [03-5450.3](#)
5. [03-8757.3](#)
6. [04-5451.3](#)
7. [04-10453.3](#)
8. [05-5460.3](#)
9. [05-10456.8](#)
10. [06-5468.2](#)
11. [06-10459.6](#)
12. [07-5477.2](#)
13. [07-10462.8](#)
14. [08-5480.1](#)
15. [08-10466.3](#)
16. [09-5482.5](#)
17. [09-10469.8](#)
18. [10-5483.5](#)
19. [10-10472.4](#)
20. [11-5485.5](#)
21. [11-9107](#)
22. [12-8065.5](#)
23. [12-10046.6](#)
24. [13-8066.9](#)
25. [13-10053.0](#)
26. [14-8096.3](#)
27. [14-16470.9](#)
28. [15-8070.3](#)
29. [15-16475.3](#)
30. [16-8.071.3](#)
31. [16-16478.2](#)
32. [17-8072.4](#)
33. [17-16483.6](#)
34. [18-9107](#)

35. [18-16488.5](#)
36. [19-9107](#)
37. [19-16492.4](#)
38. [20-8073.4](#)
39. [20-16499.2](#)
40. [21-8074.4](#)
41. [21-16503.0](#)
42. [22-8077.1](#)
43. [22-9107](#)
44. [23-8084.2](#)
45. [23-16507.0](#)
46. [24-5449.49](#)
47. [24-16510.6](#)
48. [25-5451.4](#)
49. [25-16515.2](#)
50. [26-5453.55](#)
51. [26-16519.8](#)
52. [27-4617.34](#)
53. [27-5454.23](#)
54. [28-4617.98](#)
55. [28-5455.61](#)
56. [29-4619.18](#)
57. [29-5457.78](#)
58. [30-4619.96](#)
59. [30-5459.74](#)
60. [31-4621.39](#)
61. [31-5461.95](#)
62. [32-9107](#)
63. [33-5464.02](#)
64. [34-5966.24](#)
65. [35-12285.7](#)
66. [36-12290.9](#)
67. [37-12296.1](#)
68. [38-12301.3](#)
69. [39-12306.5](#)
70. [40-12311.7](#)
71. [41-9107](#)
72. [42-9107](#)
73. [43-7889.3](#)
74. [44-7890.3](#)
75. [45-7893.](#)
76. [46-7894.6](#)
77. [47-7896.0](#)
78. [48-7897.6](#)
79. [49-7898.6](#)
80. [50-7899.6](#)
81. [51-7905.2](#)
82. [52-7907.4](#)
83. [53-8904.2](#)
84. [54-8907.6](#)

85. [55-8911.5](#)
86. [56-8915.1](#)
87. [57-8918.6](#)
88. [58-8922.2](#)
89. [59-8925.3](#)
90. [60-8928.4](#)
91. [61-12030.4](#)
92. [62-12035.0](#)
93. [63-9107](#)
94. [64-9107](#)
95. [65-12038.3](#)
96. [66-12042.8](#)
97. [67-12046.5](#)
98. [68-9306.9](#)
99. [69-9309.5](#)
100. [70-9312.6](#)
101. [71-9314.8](#)
102. [72-9317.1](#)
103. [73-9319.4](#)
104. [74-9322.0](#)
105. [75-9324.3](#)
106. [76-10281.0](#)
107. [77-10286.9](#)
108. [78-9107](#)
109. [79-10287.9](#)
110. [80-10293.5](#)
111. [81-10299.3](#)
112. [82-10612.4](#)
113. [83-10618.2](#)
114. [84-10624.2](#)
115. [85-10625.5](#)
116. [86-10636.4](#)
117. [87-9107](#)
118. [88-9107](#)
119. [10641.9](#)
120. [90-10647.9](#)
121. [91-10654.8](#)
122. [92-10660.1](#)
123. [93-10666.6](#)
124. [94-8740.6](#)
125. [95-8742.7](#)
126. [96-8745.7](#)
127. [97-8747.9](#)
128. [98-8750.7](#)
129. [99-8753.5](#)